

Exploring the influence of patient variability on propofol target-controlled infusion performance

Ylva Wahlquist^{1,*}, Amanda Gustafsson¹, and Kristian Soltesz^{1,*}

Abstract— Target-controlled infusion (TCI) constitutes a clinically available alternative to manually administering the infusion rate of the anesthetic drug propofol. In TCI, a drug infusion profile is optimized to track a reference trajectory of blood plasma or effect site (brain cortex) drug concentration, or a corresponding clinical effect. TCI is a pure feed-forward open-loop strategy, fully reliant on an underlying dynamic patient model. We show how TCI dosing of propofol—to achieve a desired depth of hypnosis—can be posed as a QP problem. We design this QP problem based on a nominal pharmacological propofol model by Eleveld et al. Then, we investigate how inter-patient variability, described as mixed effects of a particular distribution within the Eleveld model, affects TCI performance. Based on the Mahalanobis distance, we sample from probability quantiles of the mixed-effect model and evaluate the TCI designed for the nominal patient across these samples. The main outcome is that performance, in terms of achieved hypnotic depth, deteriorates to what is at the limit of clinical acceptance already when considering only 1 % of the most likely patients drawn from the uncertainty model. This is under the—for the TCI system unrealistically favorable—assumption that there is no uncertainty in the relation between effect site concentration, and clinical effect. The conclusion from the arising results is that the benefit of propofol TCI over manual dosing is unclear, even within the model that the TCI system was designed for.

Keywords: Model uncertainty, model predictive control, pharmacological modeling, target-controlled infusion

I. INTRODUCTION

Propofol is an intravenously administered anesthetic drug that affects awareness. It is commonly used as a hypnotic agent in general surgery [1], where its administration rate is governed by an infusion pump. The pump can issue constant rate infusion and brief “impulse” doses referred to as boluses. Most commonly, the issuing of boluses, and titration of the infusion rate, are achieved manually by an anesthesiologist. Dose changes are based on an assessment of how deeply anesthetized the patient is compared to what is desired. This assessment can be based on signs such as twitching, eye reflexes, changes in skin coloring or sweating; and measurements such as heart rate and blood pressure. In addition to such indirect information, there also exist monitors aimed at directly estimating hypnotic depth. The most common is the bispectral index (BIS) monitor, which outputs a real-time scalar hypnotic depth estimate based on measurements of the electroencephalogram (EEG) [2]. The

BIS scale goes between 100 (awake, fully aware) and 0 (deep anesthesia). Generally, a BIS value between 40 and 60 is desired within general surgery [3].

Along with manual dosing of propofol, there exist two automatic dosing regimens. One is closed-loop control. In this regimen, a feedback loop from BIS (or another monitor) to the infusion pump is closed over a digital computer. While this dosing regimen has been broadly studied [3]–[7], there is to date no commercially available system for closed-loop controlled infusion of propofol.

The second automatic dosing regimen is called target-controlled infusion (TCI). In TCI, a dosing profile is optimized to follow a reference effect-site (brain) or blood plasma concentration trajectory, corresponding to a given hypnotic depth [8]–[10], as characterized by the BIS scale. TCI differs from closed-loop control mainly in that no sensor feedback is used. In control system terms, TCI is therefore an feed-forward open-loop control system, as opposed to a closed-loop one [7], [11].

There exist commercial TCI systems [12], and their supporters claim that they are superior to manual dosing, since they take individual patient dynamics into account via the underlying model [8]. While closed-loop control has a natural advantage over TCI in that it relies on sensor feedback, it is also susceptible to sensor faults, and technically more complicated. It is therefore legitimate to ask: how well can we expect a TCI system to perform, in the face of model uncertainty, and the absence of sensor feedback?

In this work, we employ a state-of-the-art pharmacological model for propofol by Eleveld et al. [13]. Within it, inter-individual variability in drug response dynamics are mainly modeled by known covariates (such as body mass, age, gender, etc). The remaining variability is described by random effects, acting on the model parameters. As is common practice within pharmacological modeling [14], these random effects are modeled by a multivariate distribution from which parameters of the patient model are drawn. In this work we study how the uncertainty resulting from these random effects affects TCI performance for patients with a covariate setup that was considered to be the “reference” patient in the modeling work by Eleveld et al.

II. METHODS

We pose the TCI as a quadratic programming (QP) problem to obtain a drug infusion profile that tracks a reference trajectory of effect site (brain) drug concentration. Then, we study how a TCI system optimized for the nominal (without random effects) patient could be expected to behave. We do

¹Wahlquist, Gustafsson and Soltesz are with the Department of Automatic Control, Lund University, Sweden (e-mail: ylva.wahlquist@control.lth.se).

*This work was partially supported by the Wallenberg AI, Autonomous Systems and Software Program (WASP) funded by the Knut and Alice Wallenberg Foundation. The authors are members of the Excellence Center at Linköping-Lund in Information Technology (ELLIIT).

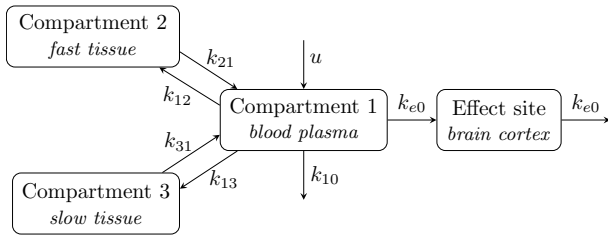


Fig. 1: Linear four-compartment model of propofol: a three-compartment model of the PK and a one-compartment PD model in (1) and (2). The input is given by the drug mass infusion rate u , while rate constants k_{ij} describe drug transfer from compartment i to j . Drug elimination from the central compartment is governed by the rate constant k_{10} and from the effect site compartment at rate k_{e0} .

this by simulating its BIS-response when inducing anesthesia on a patient model drawn from the associated inter-patient variability distribution. Using the Mahalanobis distance [15], we can draw from within likelihood quantiles, e.g., from within the 1 % of the most likely patient dynamics, and assess TCI performance across those obtained samples.

A. PKPD modeling

Pharmacokinetics (PK) refers to the uptake, distribution, and elimination of a drug in the body. The pharmacokinetics of propofol are commonly modeled by a three-compartment model [1].

Pharmacodynamics (PD) refers to the relationship between blood plasma drug concentration and the clinical effect. The pharmacodynamics for propofol are commonly modeled using two sub-models: one compartment modeling the drug concentration at the effect site (i.e., the brain) and a non-linearity relating effect site concentration to clinical effect, the hypnotic depth. Here, we consider BIS to represent the clinical effect.

Let x_i [$\mu\text{g L}^{-1}$] denote the drug concentration of the i^{th} compartment and u [$\mu\text{g min}^{-1}$] the drug mass infusion rate. We combine the PK model with the linear part of the PD model (effect-site compartment) to create the linear part of the PKPD model with four compartments. This model is shown in Figure 1, and its dynamics can be expressed in state space form as

$$\dot{\mathbf{x}} = \underbrace{\begin{bmatrix} -(k_{10} + k_{12} + k_{13}) & k_{21} & k_{31} & 0 \\ k_{12} & -k_{21} & 0 & 0 \\ k_{13} & 0 & -k_{31} & 0 \\ k_{e0} & 0 & 0 & -k_{e0} \end{bmatrix}}_A \mathbf{x} + \underbrace{\begin{bmatrix} 1 \\ \frac{1}{V_1} \\ 0 \\ 0 \end{bmatrix}}_B u, \quad (1)$$

where k_{ij} [min^{-1}] are rate constants governing drug transfer from compartment i to j and V_1 [L] is the central compartment volume. Drug elimination from the central compartment is described by the rate constant k_{10} [min^{-1}]. The

effect site concentration x_4 [$\mu\text{g L}^{-1}$] is related to the central compartment concentration x_1 by the first-order elimination rate constant k_{e0} [min^{-1}].

The nonlinear relationship between effect-site concentration and clinical effect (BIS) is commonly modeled by a sigmoid due to saturation effects at low and high concentrations. This sigmoid is often parameterized as a Hill function [3]

$$\text{BIS} = 100 \frac{C_{e,50}^\gamma}{C_{e,50}^\gamma + x_4^\gamma}, \quad (2)$$

where $C_{e,50}$ [$\mu\text{g mL}^{-1}$] is the effect site concentration at which the clinical effect is 50 % of the maximal possible, i.e., $x_4 = C_{e,50} \Leftrightarrow \text{BIS} = 50$. γ is a parameter determining the steepness of the sigmoid, and 100 is the BIS value in the absence of propofol.

It is common to describe the PK model in terms of volumes V_1, V_2, V_3 [L] and clearances CL, Q_2, Q_3 [L min^{-1}] and the conversion between these are

$$k_{10} = CL/V_1, \quad (3a)$$

$$k_{12} = Q_2/V_1, \quad (3b)$$

$$k_{13} = Q_3/V_1, \quad (3c)$$

$$k_{21} = Q_2/V_2, \quad (3d)$$

$$k_{31} = Q_3/V_3. \quad (3e)$$

If dose changes are actuated at discrete time points, with sampling period h [min], we can use the approximation-free zero-order-hold discretization

$$\mathbf{x}(k+1) = \Phi \mathbf{x}(k) + \Gamma u(k), \quad (4a)$$

of (1), where

$$\Phi = e^{Ah}, \quad (4b)$$

$$\Gamma = \int_0^h e^{A\tau} d\tau B, \quad (4c)$$

and where $\mathbf{x}(k+1)$ now indicates sample $k+1$, corresponding to $\mathbf{x}(t)$ with $t = kh + h$. We can then simulate the linear system (1) by successively computing the future state $\mathbf{x}(k+1)$ from the current state $\mathbf{x}(k)$ and drug administration $u(k)$.

B. Modeling inter-patient variability

Pharmacometric covariate modeling is a branch of pharmacology aimed at obtaining dynamical models that capture the response dynamics to a drug while accounting for inter-individual variability [13], [16]. Commonly, a Bayesian framework is used, within which the inter-individual variability in the model parameters (V_1, k_{10}, \dots) of (1) and (2) is partly explained by known covariates such as age, gender, etc, and partly by random effects.

In this study, we use the reference patient considered in Eleveld et al. [13], with covariates according to Table I. To study the effects of inter-individual variability, we fix the covariates to those of Table I, and apply random effects

TABLE I: Covariate set of the reference patient used in [13].

Covariate	Value	Unit
Age	35	year
Weight	70	kg
Height	170	cm
Added opioids	False	-
Gender	Male	-
Blood sampling	Venous	-

TABLE II: Multivariate random effect stochastic variable $\boldsymbol{\eta}$ with components $\eta_i \sim \mathcal{N}(0, \sigma_i^2)$, describing inter-individual variability of the Eleveld pharmacokinetic (PK) model [13] according to (5).

Random effect	Standard deviation (σ_i)
η_1	0.781
η_2	0.752
η_3	0.773
η_4	0.515
η_5	0.588
η_6	0.457

according to [13]. These random effects affect the PK parameters so that

$$V_1 = 6.28 \exp(\eta_1) \text{ L}, \quad (5a)$$

$$V_2 = 25.5 \exp(\eta_2) \text{ L}, \quad (5b)$$

$$V_3 = 272.9 \exp(\eta_3) \text{ L}, \quad (5c)$$

$$CL = 1.79 \exp(\eta_4) \text{ L min}^{-1}, \quad (5d)$$

$$Q_2 = 1.91 \exp(\eta_5) \text{ L min}^{-1}, \quad (5e)$$

$$Q_3 = 1.11 \exp(\eta_6) \text{ L min}^{-1}, \quad (5f)$$

where the random effects are modeled by the variables η_i for $i = 1, \dots, 6$, with $\eta_i \sim \mathcal{N}(0, \sigma_i^2)$. The standard deviations σ_i are given in Table II.

In some PKPD models, such as the Eleveld model [13], the PD parameters are also modeled with parameter uncertainty. We have chosen to keep the PD parameters fixed at their nominal values, as this is the case for most PKPD models for propofol [1]. Table III shows the PD parameters from [13], also used in this paper.

C. TCI as a quadratic program (QP)

The objective of the TCI algorithm is to optimize a drug infusion profile to follow a reference effect-site concentration trajectory.

The drug concentrations within the effect-site compartment across a horizon of N samples are

$$\boldsymbol{\chi} = \begin{bmatrix} x_4(1) & \dots & x_4(N) \end{bmatrix}^\top, \quad (6)$$

TABLE III: Parameters for the pharmacodynamic (PD) model, according to (1) and (2), of the reference patient in the Eleveld model [13].

Parameter	Value	Unit
$C_{e,50}$	3.08	$\mu\text{g mL}^{-1}$
k_{e0}	0.146	min^{-1}
γ	1.47	-

where the indices from now on indicate sample number, instead of time as in (4). Letting

$$\boldsymbol{r} = \begin{bmatrix} r(1) & \dots & r(N) \end{bmatrix}^\top \quad (7)$$

be the desired (reference) trajectory of the effect-site concentration x_4 , we seek a drug infusion profile

$$\boldsymbol{u} = \begin{bmatrix} u(1) & \dots & u(N) \end{bmatrix}^\top, \quad (8)$$

that minimizes the quadratic cost function

$$\begin{aligned} J'(\boldsymbol{\chi}) &= \sum_{k=1}^N (\chi(k) - r(k))^2 \\ &= (\boldsymbol{\chi} - \boldsymbol{r})^\top (\boldsymbol{\chi} - \boldsymbol{r}) \\ &= \boldsymbol{\chi}^\top \boldsymbol{\chi} - 2\boldsymbol{r}^\top \boldsymbol{\chi} + \boldsymbol{r}^\top \boldsymbol{r}. \end{aligned} \quad (9)$$

For our TCI problem, we want to minimize cost over \boldsymbol{u} , rather than over $\boldsymbol{\chi}$. Thus, we rewrite (9) in terms of \boldsymbol{u} . Assuming the initial state $\boldsymbol{x}(0) = \boldsymbol{x}_0$, we can express \boldsymbol{x} (and therefore also $\boldsymbol{\chi}$) in \boldsymbol{u} using the recursion

$$\begin{aligned} \boldsymbol{x}(1) &= \Phi \boldsymbol{x}_0 + \Gamma u(1), \\ \boldsymbol{x}(2) &= \Phi^2 \boldsymbol{x}_0 + \Phi \Gamma u(1) + \Gamma u(2), \\ &\vdots \\ \boldsymbol{x}(N) &= \Phi^N \boldsymbol{x}_0 + \Phi^{N-1} \Gamma u(1) + \dots + \Gamma u(N). \end{aligned} \quad (10)$$

Letting Φ_4 be the fourth row of Φ and Γ_4 the fourth element of Γ , we obtain

$$\begin{aligned} \chi(1) &= \Phi_4^1 \boldsymbol{x}_0 + \Phi_4^0 \Gamma_4 u(1), \\ \chi(2) &= \Phi_4^2 \boldsymbol{x}_0 + \Phi_4^1 \Gamma_4 u(1) + \Phi_4^0 \Gamma_4 u(2), \\ &\vdots \\ \chi(N) &= \Phi_4^N \boldsymbol{x}_0 + \Phi_4^{N-1} \Gamma_4 u(1) + \dots + \Phi_4^0 \Gamma_4 u(N), \end{aligned} \quad (11)$$

which we write in matrix form as

$$\boldsymbol{\chi} = \underbrace{\begin{bmatrix} \Phi_4^1 \\ \vdots \\ \Phi_4^N \end{bmatrix}}_E \boldsymbol{x}_0 + \underbrace{\begin{bmatrix} \Phi_4^0 \Gamma_4 & & & \\ \Phi_4^1 \Gamma_4 & \Phi_4^0 \Gamma_4 & & \\ \vdots & \vdots & \ddots & \\ \Phi_4^{N-1} \Gamma_4 & \Phi_4^{N-2} \Gamma_4 & \dots & \Phi_4^0 \Gamma_4 \end{bmatrix}}_F \boldsymbol{u}. \quad (12)$$

We note that E and F are constant matrices since they only depend on Φ_4 and Γ_4 , and can therefore be precomputed if several iterations of the TCI are to be performed.

Combining (9) with (12) yields

$$J'(\mathbf{u}) = (E\mathbf{x}_0 + F\mathbf{u})^\top (E\mathbf{x}_0 + F\mathbf{u}) - 2\mathbf{r}^\top (E\mathbf{x}_0 + F\mathbf{u}) + \mathbf{r}^\top \mathbf{r}. \quad (13)$$

Expanding and taking into account that the cost is scalar, we obtain

$$J'(\mathbf{u}) = \mathbf{u}^\top F^\top F\mathbf{u} + 2\mathbf{x}_0^\top E^\top F\mathbf{u} - 2\mathbf{r}^\top F\mathbf{u} + \mathbf{x}_0^\top E^\top E\mathbf{x}_0 - 2\mathbf{r}^\top E\mathbf{x}_0 + \mathbf{r}^\top \mathbf{r}. \quad (14)$$

Since the last terms are independent of \mathbf{u} and thus do not affect minimization over \mathbf{u} , we can remove those from the cost function to obtain the cost

$$J(\mathbf{u}) = \frac{1}{2}\mathbf{u}^\top F^\top F\mathbf{u} + \mathbf{x}_0^\top E^\top F\mathbf{u} - \mathbf{r}^\top F\mathbf{u}, \quad (15)$$

which therefore shares minima with $J'(\mathbf{u})$ in (14).

Next, we want to introduce constraints so that $u(k) \geq 0$ for $k = 1, \dots, N$, since drug can be intravenously added, but not actively removed. This can be expressed as \mathbf{u} being element-wise larger or equal to zero, i.e.,

$$\mathbf{u} \succeq \mathbf{0}_{N \times 1}, \quad (16)$$

where $\mathbf{0}_{N \times 1}$ is the zero vector of size N .

We want to avoid a large undershoot and stay within the recommended clinical BIS range of 40 – 60. Therefore, we limit our effect-site concentration by an upper bound, corresponding to a BIS value of 40, and add this as a constraint, so that

$$\boldsymbol{\chi} = \mathbf{x}_4 \preceq C_{e,\max} \mathbf{1}_{N \times 1}, \quad (17)$$

where $C_{e,\max}$ is the maximum allowed effect site concentration. Using (12), we can rewrite (17) as

$$E\mathbf{x}_0 + F\mathbf{u} \preceq C_{e,\max} \mathbf{1}_{N \times 1}. \quad (18)$$

Combining the two constraints (16) and (18), we arrive at the following quadratic programming (QP) problem of minimizing (15) over \mathbf{u} subject to

$$\begin{bmatrix} -I_{N \times N} \\ F \end{bmatrix} \mathbf{u} \preceq \begin{bmatrix} \mathbf{0}_{N \times N} \\ C_{e,\max} \mathbf{1}_{N \times 1} - E\mathbf{x}_0 \end{bmatrix}, \quad (19)$$

where $I_{N \times N}$ denotes the identity matrix of size $N \times N$.

This problem can be solved using standard QP solvers, such as `quadprog` in MATLAB [17], or `OSQP` available in MATLAB, Python, and Julia [18].

D. Uncertainty quantile sampling

Now that we can solve the TCI optimization problem, we move on to study how a TCI system, optimized for the nominal patient, behaves in the face of inter-individual PK variability, characterized by the Eleveld random effect model. For example, if we want to study the 1 % likelihood quantile of “most likely patients”, we need to sample from a subset of the random effect model corresponding to 1 % of the probability mass. This probability mass is chosen to contain the most likely values of the underlying random variable. To do this, we will use uncertainty quantile sampling.

The parameter uncertainty described by random effects in the Eleveld model follows a multivariate normally distributed variable $\boldsymbol{\eta} \sim \mathcal{N}(\mathbf{0}, \boldsymbol{\Sigma})$, with variance-covariance matrix $\boldsymbol{\Sigma} = \text{diag}[\sigma_1 \dots \sigma_n]$ according to Table II.

The likelihood of a sample $\boldsymbol{\eta}_s$ of $\boldsymbol{\eta}$ is

$$l(\boldsymbol{\eta}_s) = \frac{\exp(-\frac{1}{2}m(\boldsymbol{\eta}_s))}{\sqrt{(2\pi)^n \det \boldsymbol{\Sigma}}}, \quad (20a)$$

$$m(\boldsymbol{\eta}_s) = \boldsymbol{\eta}_s^\top \boldsymbol{\Sigma}^{-1} \boldsymbol{\eta}_s, \quad (20b)$$

where the right-hand-side of (20a) is the probability density function (PDF) of $\mathcal{N}(\mathbf{0}, \boldsymbol{\Sigma})$ evaluated at $\boldsymbol{\eta}_s$. The number of PK parameters are $n = 6$, and $m(\cdot)$ of (20b) defines the squared Mahalanobis distance [15].

Since our normal PDF has a unique mode at $\mathbf{0}$ and is strictly monotonously decreasing in $\|\boldsymbol{\eta}_s\|$, the likelihood $l(\cdot)$ defines a sequence of unique and closed level surfaces, such that each point interior to a level surface has a higher probability than points on the level surface, while each point exterior to a level surface has a lower likelihood than points at the level surface. The level surface containing $\boldsymbol{\eta}_s$ can thus be used to uniquely partition the support of $\boldsymbol{\eta}$ into a set of points with a likelihood larger than or equal to $l(\boldsymbol{\eta}_s)$, and one set of points with a likelihood smaller than $\boldsymbol{\eta}$.

To sample from the α -quantile of most likely $\boldsymbol{\eta}$, we thus have to find the level surface enclosing points corresponding to a fraction α of the total probability mass. The sought surface can be conveniently determined using the squared Mahalanobis distance (20b), which has the property that each point at the level surface that goes through $\boldsymbol{\eta}_s$ shares the Mahalanobis distance with $\boldsymbol{\eta}_s$. The Mahalanobis distance thus constitutes a generalization of the univariate Gaussian standard deviation to the multivariate case.

A convenient property of the squared Mahalanobis distance is that it follows the χ^2 -distribution of order n , as explained in [19]. To find the squared Mahalanobis distance m_α corresponding to our sought α -quantile we thus (numerically) find the unique solution m_α of

$$P(m(\boldsymbol{\eta}_s) \leq m_\alpha) = \alpha = \int_0^{m_\alpha} \frac{m^{(n-2)/2} e^{-m/2}}{2^{m/2} \Gamma(n/2)} dm, \quad (21)$$

where the right-hand-side is the cumulative distribution function (CDF) of the mentioned χ^2 -distribution.

Finally, to sample from the α -quantile of interest, we first sample $\boldsymbol{\eta}_s$ from $\boldsymbol{\eta}$. If $m(\boldsymbol{\eta}_s) \leq m_\alpha$ we keep the sample; else we repeat until we obtain a sample that fulfills this inequality.

E. Simulation example

We investigate how random effects in the PK parameters affect TCI performance. Particularly, we consider the induction phase of anesthesia, during which a propofol infusion profile is optimized to transition the patient from the fully aware state of BIS 100 to the desired anesthetic depth of BIS 50. This transition should be as fast as possible while avoiding undershoots below BIS 40, or subsequent overshoots exceeding BIS 60 [3].

In our formulation from Section II-C, this corresponds to fixing the reference trajectory r at the effect site concentration equivalent of BIS 50. To avoid the mentioned undershoot, we chose the maximum allowed effect site concentration $C_{e,max}$ to the value that corresponds to a BIS value of 40. Note that both the reference and the undershoot limit are for the nominal patient, in the absence of random effects.

To assess how inter-individual variability affects TCI performance, we generate a set of 1000 models by sampling from the random effect uncertainty model in (5), and apply the propofol trajectory optimized to the nominal patient model to each of them. Specifically, we sample from the 50 % and 1 % quantile ($\alpha = 0.5$ and $\alpha = 0.01$, respectively) using the quantile sampling method described in Section II-D.

To achieve this, we implemented our methodology in the programming language Julia and employed the QP solver OSQP [18] to (15). The code is available in [20].

III. RESULTS

Figure 2 shows the propofol infusion profile u optimized for the nominal patient, while the resulting BIS response for the nominal patient is shown in Figure 3 in red. The infusion profile commences with a bolus that makes the nominal patient BIS approach the reference of BIS 50, minimizing the cost function (15). Since infusion rates cannot be negative, this bolus is followed by an episode of zero infusion over the next few minutes. After this, the infusion profile changes to balance out the effect of drug elimination that would otherwise make the BIS deviate from its reference level.

Using the sampling strategy of Section II-D, we have then simulated 1000 patient models each sampled from the 50 % and 1 % quantiles, with results shown as blue curves in Figure 3.

To further characterize the spread in responses for these quantiles, we have drawn their steady-state distributions (i.e., their spread at 10 min in Figure 3) in Figure 4. The dashed black lines in Figure 3 and Figure 4 indicate the clinically recommended BIS range, as mentioned in Section I.

Code examples reproducing all results are available in [20].

IV. DISCUSSION

Figure 3 shows that inter-patient variability of the Elefeld PK model [13] affects TCI performance notably. When individuals are selected from the 50 % model uncertainty quantile, the resulting range of BIS values is large. This can be seen in Figure 3a where 34 % of the drawn patients have stationary BIS values that fall outside the clinically recommended 40–60 range. To ensure that 99 % of the drawn patients fall within the recommended range, we need to delimit sampling to within the 1 % quantile, as seen in Figure 3b.

The spread of induction phase profiles in Figure 3 suggests that there is a considerable spread not only in the steady-state, but also in the preceding transient. As a result, the

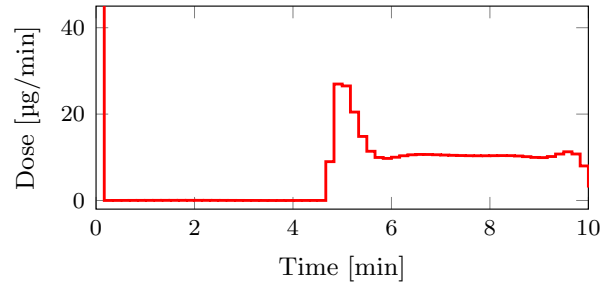
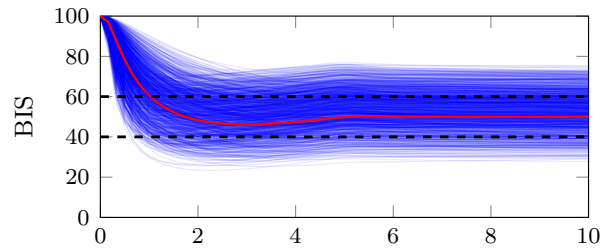
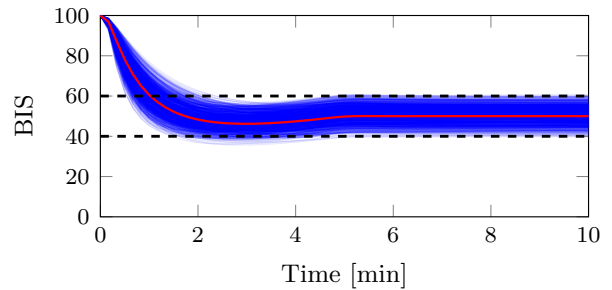


Fig. 2: Propofol infusion profile computed by the TCI algorithm for the considered nominal patient. The initial bolus is capped, to resolve the subsequent infusion profile. The drug amount provided in this bolus is 9.7 mg.



(a) 50 % most likely patients



(b) 1 % most likely patients

Fig. 3: Simulated responses across samples from the 50 % (a) and 1 % (b) most likely patients, drawn from the distributions of the PK random effect vector η , cf. Table II and (5). The input is the drug profile in Figure 2. Red curves show the response for the nominal patient, on which the TCI design was based. Horizontal dashed curves show the bounds of the clinically recommended BIS range.

possible motivation to use TCI systems to improve transient behavior could be questioned.

That inter-patient variability has a negative impact on TCI performance should in itself not come as a surprise, since TCI is a pure open-loop control regimen. However, the extent of this degradation, as indicated by Figure 3 and Figure 4 is concerning.

When administering propofol using a TCI algorithm, there is an anesthesiologist present, just like in the case of manual dosing. This means that the anesthesiologist can intervene if there are signs of under- or overdosing. Instead of changing the infusion rate directly, the anesthesiologist will now instead change the reference concentration of the TCI

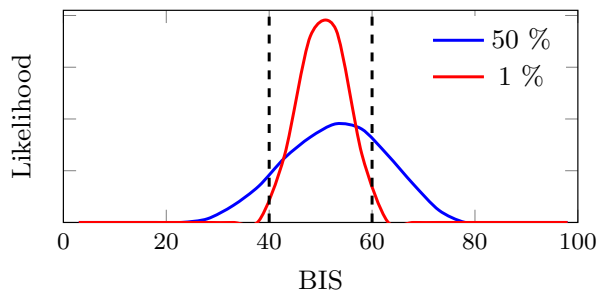


Fig. 4: Expected distribution of the steady-state BIS values across from the 50 % (blue) and 1 % (red) most likely patients, drawn from the distributions of the PK random effect vector η , cf. Table II and (5). I.e., the range of BIS values at $t = 10$ min in Figure 3. Vertical dashed lines indicate the clinically recommended BIS range.

system. Since a higher reference concentration will result in a higher drug infusion rate, this mechanism enables accounting for inter-patient variability, just like manual dose changes would. These event-driven dose changes make it challenging to make fair comparisons between manual dosing and TCI in a clinically realistic setting. This prompted our investigation of TCI in a simulation setting where it is employed in the model it was designed for in the first place.

Our study focuses on how random effect variability of the PK parameters affects the TCI. However, in some PKPD models, such as the Eleveld model [13], the PD parameters are also associated with random effects. We have chosen to keep the PD model fixed at its nominal parameter values. Including their variability in the analysis would further increase the already concerning range of the expected BIS in Figure 3 and Figure 4. For instance, if we add random effects to the PD parameters according to the Eleveld model [13], and draw from the 50 % quantile, we obtain that 50 % of the steady-state BIS values are outside the clinically feasible 40–60 range.

BIS-guided closed-loop dosing solutions has shown promising clinical results [5], [21]. However, it only works well if the BIS signal is reliable, but suffer issues when feedback signal quality is poor. In the extreme case of total signal loss, TCI would then be the best choice for setting drug infusion. We are currently working on exploiting this insight and devising a state-observer-based hybrid between closed-loop control and TCI, which smoothly transitions between the two based on a scalar signal quality index (SQI), provided by the BIS and other clinically available monitors [22].

V. CONCLUSIONS

TCI, in the absence of manual reference adjustments, can merely maintain clinically acceptable performance when taking into account as little as the 1 % most likely fraction of the population. Therefore, the main conclusion of our work is that it can be questionable whether these TCI systems come with a clinical advantage over manual dosing, based on that the models were designed for these systems in the first place.

REFERENCES

- [1] M. M. Sahinovic, M. M. R. F. Struys, and A. R. Absalom, "Clinical pharmacokinetics and pharmacodynamics of propofol," *Clinical Pharmacokinetics*, vol. 57, no. 12, pp. 1539–1558, 2018.
- [2] J. C. Sigl and N. G. Chamoun, "An introduction to bispectral analysis for the electroencephalogram," *Journal of Clinical Monitoring*, vol. 10, no. 6, pp. 392–404, 1994.
- [3] S. Bibian, C. R. Ries, M. Huzmezan, and G. Dumont, "Introduction to automated drug delivery in clinical anesthesia," *European Journal of Control*, vol. 11, no. 6, pp. 535–557, 2005.
- [4] G. A. Dumont, A. Martinez, and J. M. Ansermino, "Robust control of depth of anesthesia," *International Journal of Adaptive Control and Signal Processing*, vol. 23, no. 5, pp. 435–454, 2009.
- [5] K. van Heusden, G. A. Dumont, K. Soltesz, C. L. Petersen, A. Umedaly, N. West, and J. M. Ansermino, "Design and clinical evaluation of robust pid control of propofol anesthesia in children," *IEEE Transactions on Control Systems Technology*, vol. 22, no. 2, pp. 491–501, 2014.
- [6] F. Padula, C. Ionescu, N. Latronico, M. Paltenghi, A. Visioli, and G. Vivacqua, "Optimized PID control of depth of hypnosis in anesthesia," *Computer Methods and Programs in Biomedicine*, vol. 144, pp. 21–35, 2017.
- [7] A. Gustafsson, "Towards individualised anaesthesia: A comparison between target-controlled infusion and closed-loop control," 2023. Master thesis report TFRT-6217. Lund University, Department of Automatic Control.
- [8] S. L. Shafer and K. M. Gregg, "Algorithms to rapidly achieve and maintain stable drug concentrations at the site of drug effect with a computer-controlled infusion pump," *Journal of Pharmacokinetics and Biopharmaceutics*, vol. 20, no. 2, pp. 147–169, 1992.
- [9] A. R. Absalom, J. I. B. Glen, G. J. C. Zwart, T. W. Schnider, and M. M. R. F. Struys, "Target-controlled infusion: A mature technology," *Anaesthesia & Analgesia*, vol. 122, no. 1, p. 70, 2016.
- [10] D. Mehta, J. McCormack, P. Fung, G. Dumont, and J. M. Ansermino, "Target controlled infusion for Kids: Trials and simulations," in *2008 30th Annual International Conference of the IEEE Engineering in Medicine and Biology Society*, pp. 5818–5821, 2008.
- [11] K. J. Åström and R. M. Murray, *Feedback Systems : An Introduction for Scientists and Engineers*. Princeton University Press, 2008.
- [12] J. B. Glen, "The development of 'Diprifusor': A TCI system for propofol," *Anaesthesia*, vol. 53, no. s1, pp. 13–21, 1998.
- [13] D. J. Eleveld, P. Colin, A. R. Absalom, and M. M. R. F. Struys, "Pharmacokinetic–pharmacodynamic model for propofol for broad application in anaesthesia and sedation," *British Journal of Anaesthesia*, vol. 120, pp. 942–959, May 2018.
- [14] L. B. Sheiner, B. Rosenberg, and V. V. Marathe, "Estimation of population characteristics of pharmacokinetic parameters from routine clinical data," *Journal of Pharmacokinetics and Biopharmaceutics*, vol. 5, no. 5, pp. 445–479, 1977.
- [15] P. C. Mahalanobis, "On the generalized distance in statistics," *Proceedings of the National Institute of Sciences (Calcutta)*, vol. 2, pp. 49–55, 1936.
- [16] Y. Wahlquist, J. Sundell, and K. Soltesz, "Learning pharmacometric covariate model structures with symbolic regression networks," *Journal of Pharmacokinetics and Pharmacodynamics*, 2023.
- [17] MathWorks, "quadprog," 2023. <https://se.mathworks.com/help/optim/ug/quadprog.html>.
- [18] B. Stellato, G. Banjac, P. Goulart, A. Bemporad, and S. Boyd, "OSQP: An operator splitting solver for quadratic programs," *Mathematical Programming Computation*, vol. 12, no. 4, pp. 637–672, 2020.
- [19] R. De Maesschalck, D. Jouan-Rimbaud, and D. L. Massart, "The Mahalanobis distance," *Chemometrics and Intelligent Laboratory Systems*, vol. 50, no. 1, pp. 1–18, 2000.
- [20] Y. Wahlquist, "tci-variability," <https://github.com/wahlquist/tci-variability>. Commit: 1c4867b, 2023.
- [21] M. Schiavo, F. Padula, N. Latronico, L. Merigo, M. Paltenghi, and A. Visioli, "Performance evaluation of an optimized PID controller for propofol and remifentanyl coadministration in general anaesthesia," *IFAC Journal of Systems and Control*, vol. 15, p. 100121, 2021.
- [22] N. Liu, T. Chazot, A. Genty, A. Landais, A. Restoux, K. McGee, P.-A. Laloë, B. Trillat, L. Barvais, and M. Fischler, "Titration of propofol for anesthetic induction and maintenance guided by the bispectral index: Closed-loop versus manual control," *Anesthesiology*, vol. 104, no. 4, pp. 686–695, 2006.